LIMITS ON CHROMOSPHERES AND CONVECTION AMONG THE MAIN-SEQUENCE A STARS[1]

Theodore Simon

Institute for Astronomy, University of Hawaii, 2680 Woodlawn Drive, Honolulu, HI 96822

Thomas R. Ayres

Center for Astrophysics and Space Astronomy, 389 UCB, University of Colorado, Boulder, CO 80309

AND

Seth Redfield and Jeffrey L. Linsky

JILA, 440 UCB, University of Colorado, Boulder, CO 80309

Received 2002 May 7; accepted 2002 July 17

ABSTRACT

In deeply convective stars, the nonthermal energy required to heat the chromosphere ultimately is supplied by turbulent magnetoconvection. Because the early and middle A stars have very shallow convective layers, they are not expected to produce enough magnetoconvective power to sustain luminous chromospheres or hot coronae. Here we describe a search for chromospheric emission in the far-ultraviolet (905–1185 Å) spectra of seven main-sequence A stars, based on observations from the *Far Ultraviolet Spectroscopic Explorer* (*FUSE*) telescope. Our survey spans the interval in effective temperature along the main sequence over which powerful subsurface convection zones and hence chromospheric emission are expected to vanish. The presence or absence of high-temperature emissions in our *FUSE* spectra therefore can be used to identify the locus for the transition from convective to radiative envelopes—a change in stellar structure that is difficult to assess by other means. We present our observations and analysis of the subcoronal emission lines of C III $\lambda\lambda$977, 1175 and O VI $\lambda\lambda$1032, 1037, which bracket a range in formation temperatures from 50,000 to 300,000 K. To supplement our *FUSE* observations, we also report Goddard High Resolution Spectrograph measurements of Si III λ1206 and H I Lyα λ1215, obtained from archival observations of the *Hubble Space Telescope*, as well as X-ray measurements from previous *ROSAT* survey and pointed observations. We detected C III and O VI emission features in the *FUSE* spectra of the coolest stars of our sample, at $T_{\rm eff} \lesssim 8200$ K. When normalized to the bolometric luminosities, the detected emission-line fluxes are comparable to solar values. We detected none of the hotter stars in our survey at $T_{\rm eff} \geq 8300$ K. Upper limits on the normalized flux in some instances approach 40 times less than solar. Within an uncertainty in the effective temperature scale of up to several hundred kelvins, our *FUSE* observations indicate that the transition between convective and radiative stellar envelopes takes place at, or very near, the point along the main sequence where stellar structure models predict and, moreover, that the changeover occurs very abruptly, over a temperature interval no greater than $\sim$100 K in width. Our *FUSE* sample also includes two binary stars. In both cases, the narrow UV line profiles we have observed suggest that the high-temperature emission is most likely associated with the late-type companions rather than the A stars themselves.

Subject headings: stars: activity — stars: chromospheres — stars: late-type — ultraviolet: stars

1. INTRODUCTION

According to stellar structure models, the main-sequence A stars have very shallow subsurface convection zones (Latour 1970; Richer, Michaud, & Proffitt 1992; Castelli, Gratton, & Kurucz 1997; Christensen-Dalsgaard 2000). For that reason, A stars are not expected to have high-temperature chromospheres or coronae, which exist only when turbulent (magneto-) convection is present to supply the nonthermal energy needed for heating (e.g., Parker 1970). Thus, the very thinly convective early and middle A stars are not expected to be intense sources of coronal X rays or to radiate strongly in chromospheric spectral lines at ultraviolet (UV) wavelengths. A small handful of such stars have nonetheless been detected in X rays by the *Einstein Observatory* or by *ROSAT* (e.g., Schmitt et al. 1985; Simon, Drake,

& Kim 1995), but in those cases the observed emission is thought to come from spatially unresolved late-type binary companions or neighboring stars within the X-ray beam, not from the A stars themselves (Golub et al. 1983). A small number of chemically peculiar Bp and Ap stars have also been detected as X-ray sources. In those cases, too, the observed emission is believed to originate from a late-type companion or to be magnetospheric in origin rather than coronal (Drake et al. 1994).

UV spectroscopy has proved to be less prone to the ambiguities arising from source confusion than X-ray imaging and has been used extensively to investigate chromospheric activity throughout the H-R diagram. Among the published studies of main-sequence stars are several deep surveys of the early F stars and the late A stars. In the wavelength region longward of Lyα, for example, UV spectra from the *International Ultraviolet Explorer* (*IUE*) spacecraft have established that intense chromospheres—and, by implication, very powerful subphotospheric convection zones—are common among the early F stars. In terms of their chromo-

spheric fluxes at UV wavelengths, the F stars resemble moderately to strongly active solar-type G and K dwarfs or giants (e.g., Simon & Landsman 1991).

At earlier spectral types, the photospheric energy distribution longward of Lyα grows increasingly bright until, among the A-type stars, the diagnostically important chromospheric and subcoronal lines of C II (1335 Å), Si IV (1400 Å), and C IV (1550 Å) no longer can be detected against the intense background. However, in the region around Lyα, and especially at wavelengths below it, an A star photosphere is very dark, owing to the presence of strong absorption edges of atomic carbon. Observing in this wavelength region has made it possible to extend the blueward boundary for chromospheres from the early F stars into the middle A stars. In particular, spectra of the mid-A star τ^3 Eri, taken with the Goddard High Resolution Spectrograph (GHRS) on the *Hubble Space Telescope* (*HST*), display chromospheric emission in both Lyα and Si III λ1206. At $B-V = 0.16$, τ^3 Eri is the hottest main-sequence star we know to have a chromosphere and thus an outer convection zone (Simon & Landsman 1997). This observational boundary limit approaches tentatively close to the theoretical locus for the transition from radiative to convective envelopes near $T_{\rm eff} = 8300$ K, or $B-V = 0.14$, among the middle or early A stars (e.g., Castelli et al. 1997; Christensen-Dalsgaard 2000).

The far-ultraviolet (FUV) wavelengths below Lyα offer even greater advantages for chromospheric observations of the early A stars but have not been accessible to *HST* owing to its short-wavelength cutoff at 1150 Å. Limited observations of stellar chromospheres were made in that part of the spectrum during the *ORFEUS-SPAS II* space shuttle mission in 1996, including a pointing on the A7 V star α Cep (Simon & Ayres 1998). Even for that bright 2d magnitude star, a true stellar continuum at FUV wavelengths was weak or absent, consistent with Kurucz line-blanketed models. The strongest stellar features in the *ORFEUS* spectrum were Si III λ1206, C III λ1175, and O VI λλ 1032, 1037. In the Sun, the same features originate from the chromosphere and the so-called chromosphere-corona transition region at temperatures in the range $\sim 2 \times 10^4$ to $\sim 3 \times 10^5$ K. Normalized to the stellar bolometric luminosity, the strengths of the FUV lines recorded for α Cep were within a factor of 2 of the corresponding values for the full disk of the Sun at a time of moderate solar activity. Thus, despite the theoretical presumption that an A-type star like α Cep has only a minimal convection zone, the UV evidence demonstrates that the convection in such a star is able to maintain chromospheric activity at a level comparable to that of much more deeply convective stars, including the Sun.

As a confirmation of the physics underlying the current generation of models of stellar interiors and evolution, it is important to establish whether the boundary line for stellar convection, as represented by τ^3 Eri, has been correctly identified or whether the transition between radiative and convective envelopes lies higher up the main sequence, possibly among the very early A stars or perhaps even among the late B stars (some of which have also been detected as X-ray sources: e.g., Cassinelli et al. 1994; Schmitt et al. 1993; Grillo et al. 1992). To that end, we have undertaken the first FUV survey of main-sequence A stars, using the *FUSE* observatory to explore the wavelengths below Lyα, where the faintness of an A star photosphere greatly improves the

chances of detecting weak chromospheric emission. This paper reports the initial results of our survey.

2. OBSERVATIONS

2.1. *The FUSE A Star Sample*

Our *FUSE* sample is comprised of seven stars whose $B-V$ colors and effective temperatures span the range along the main sequence where convection zones—and hence UV chromospheric and transition region emission lines—are expected to vanish, i.e., where theory predicts a transformation from deeply convective envelopes to radiative ones. The $B-V$ colors of our program stars range from 0.22 to 0.05, while the effective temperatures range from 7800 to 8600 K (as estimated from Strömgren photometry), thus straddling the current boundary line for chromospheric emission and convection. We have concentrated on stars having "normal" (i.e., solar-like) chemical abundances because we are most interested here in stars that promise the best insight into the origin of chromospheric and coronal activity on the Sun. Two recent studies of the Mg II lines of late-type giants and dwarfs find no connection between chromospheric fluxes and metallicity, at least for activity levels comparable to that of the quiet Sun (Cuntz, Rammacher, & Ulmschneider 1994; Peterson & Schrijver 1997). Furthermore, the numerical calculations of Ulmschneider et al. (1999) demonstrate that the amount of wave energy generated by convection in main-sequence stars is independent of the metal abundance for stars of the Sun's temperature or higher (because most of the nonthermal energy is then generated in the outermost layers of the convection zone, where hydrogen is mostly ionized and also is a major source of opacity). We note, however, that the Ulmschneider et al. study did not address the separate but equally important question of whether the abundances have any effect on the propagation and dissipation of waves below and within the chromosphere itself. As for magnetic heating models, we are not aware of any theory that, starting from first principles, offers any guidance as to how the chromospheric activity of a star might change with metallicity.

A summary of the relevant parameters of the stars that we observed with *FUSE* can be found in Table 1. Spectral types are from the work of Gray & Garrison (1987, 1989). The remaining information was extracted from the SIMBAD database, except for the effective temperatures ($T_{\rm eff}$) given in the final column, which we derived from the four-color photometry. For that calculation we used the "uvbybeta" procedure from the IDL Astronomy User's Library (Landsman 1993),[2] which follows the precepts of Moon & Dworetsky (1985). Our $T_{\rm eff}$ estimates lie within a few hundred kelvins of the values that were derived independently by Allende Prieto & Lambert (1999) from stellar evolutionary calculations and those that were obtained by Sokolov (1995) from the slope of the Balmer continuum between 3200 and 3600 Å.

Two stars in our sample are noted as binaries in the SIMBAD database; the others we presume to be single, although naturally we cannot be certain of the fact. β Ari is a double-lined spectroscopic binary in a highly eccentric orbit with a 107 day period (Tomkin & Tran 1987). The spectral type and mass of the secondary component are esti-

[2] See http://idlastro.gsfc.nasa.gov.

TABLE 1
STARS OBSERVED BY *FUSE*

Name	HD	HIP	Spectral Type	$v \sin i$ (km s^{-1})	V	B−V	π (mas)	M_v	$L_{bol}/L_\odot$	β	b−y	T_{eff} (K)
ι Cen	115892	65109	A2 Va	75	2.75	0.05	55.64	1.48	20.1	2.901	0.004	8630
β Leo	102647	57632	A3 Va	115	2.14	0.09	90.16	1.92	13.0	2.899	0.043	8590
β Ari	11636	8903	A4 V	70	2.64	0.13	54.74	1.33	21.9	2.879	0.059	8400
δ Leo	97603	54872	A4 IV	180	2.56	0.12	56.52	1.32	22.1	2.869	0.067	8300
τ^3 Eri.........	18978	14146	A4 V	120	4.09	0.16	37.85	1.98	12.0	2.858	0.091	8210
ι UMa	76644	44127	A7 IVn	140	3.14	0.19	68.32	2.31	8.8	2.843	0.104	8060
α Cep	203280	105199	A7 Vn	205	2.44	0.22	66.84	1.57	17.6	2.807	0.127	7840

mated by Tomkin & Tran and also by Pan et al. (1990) to be late F or early G and ~1.2 $M_\odot$, respectively. The difference in brightness between the primary and secondary is a factor of 15 or more. The other binary star in our sample, ι UMa, is the visual triple system ADS 7114 (=CCDM J08592+4803). The bright A star primary (component A) is accompanied by a pair of 10th magnitude dM stars (the B and C components). The BC separation is on the order of 0″.5. The A–BC separation was last measured as ~5″ in 1961 (Worley 1962; Van Biesbroeck 1974) and possibly closing (Eggen 1956).

2.2. The FUSE Pointings

The individual *FUSE* observations are listed in Table 2. The *FUSE* spacecraft and its instrumentation are described by Moos et al. (2000) and Sahnow et al. (2000). Each observation was acquired in the normal time-tag mode through the large science aperture (LWRS: 30″ × 30″). We processed the raw data sets using version 2.0.5 of the CalFUSE calibration software, screening the photon lists and adjusting the calibrated spectra to compensate for a variety of instrumental signatures. For example, the accepted "good time intervals" exclude the times of burst events as well as the times when it seemed likely that guiding errors resulted in a significant loss of signal in one or more spectral channels. Two integration times are listed for each star, the first for the full exposure, the second for just the nighttime portion of the *FUSE* orbit, which normally experiences a much lower level of contamination by terrestrial airglow (Feldman et al. 2001). Except in the case of α Cep, however, the nighttime spectra are underexposed so they were used mainly as a consistency check and as an aid for estimating the errors in the spectral line fluxes that we quote below.

Figure 1 presents composite spectra for the stars in our *FUSE* sample, arranged in the order of decreasing T_{eff}. The spectrum of α Cep is based on the nighttime data taken for that star. The plots for the remaining stars are derived from the full data sets. Because the original CalFUSE output are highly oversampled (by a factor of 8), we have smoothed the spectra in Figure 1 to a resolution of ~0.05 Å. The brightest airglow lines are marked in the upper panels of the figure; the most prominent high-temperature stellar lines are identified in the lower panels. The "cleanest" stellar lines in our A star spectra are C III λ977, O VI λ1032, and the C III λ1175 multiplet, judging by a comparison with the very high quality *FUSE* spectrum of Capella that was published by Young et al. (2001). O VI λ1037, the weaker component of the O VI doublet, is also seen in Figure 1. However, in the high signal-to-noise ratio spectrum of Capella, that line is blended with both an airglow feature and the redward component of the stellar C II $\lambda\lambda$1036, 1037 doublet. Excluding α Cep, the signal-to-noise ratios of our observations are too low to establish whether those same features are present in our data.

The integrated line fluxes and their associated 1 σ errors, or the appropriate flux upper limits, were measured for each star. The results are summarized in Table 3. No corrections have been made for interstellar extinction, nor should they be needed for such nearby stars. The long-wavelength continua of the hottest stars in our sample, ι Cen and β Leo, are too bright for us to set a meaningful limit on the strength of C III λ1175. The line fluxes tabulated for α Cep are in reasonable agreement with the earlier results of Simon & Ayres (1998), considering the lower sensitivity and spectral resolution of the *ORFEUS* observation. There is no evidence for any long-term variability of that star.

TABLE 2
JOURNAL OF *FUSE* OBSERVATIONS

Star Name	FUSE Data Set	UT Date	Start Time	Exp. Time[a] (ks)	Night Only[a] (ks)
ι Cen	a0410505000	2000 Jul 09	03:28:14	13.8	8.6
β Leo	a0410202000	2001 Apr 17	01:13:46	7.4	4.0
β Ari	a0410101000	2001 Sep 03	21:07:29	10.0	2.8
δ Leo	a0410303000	2000 Dec 21	02:44:26	7.9	1.9
τ^3 Eri..........	a0410606000	2001 Aug 06	21:53:42	12.8	3.0
ι UMa	a0410405000	2001 Nov 04	15:16:42	5.9	1.7
α Cep	a0410707000	2000 Aug 12	07:11:54	27.6	15.7
α Cep	a0410708000	2000 Aug 12	20:46:24	25.8	12.6

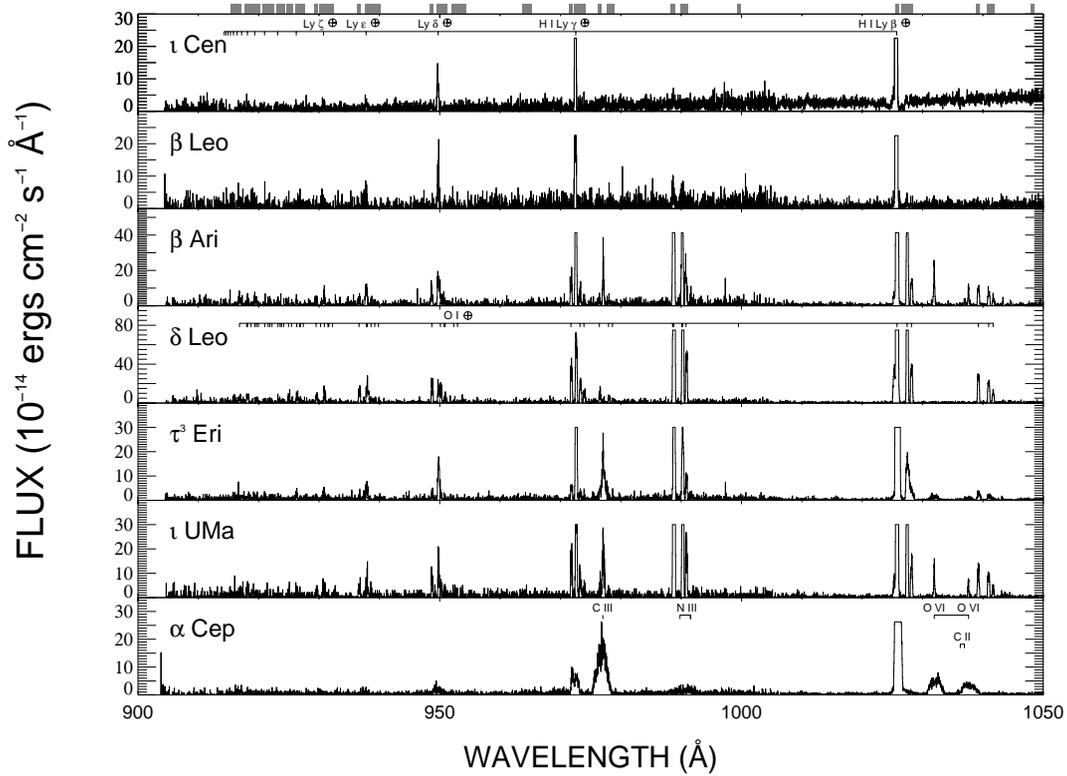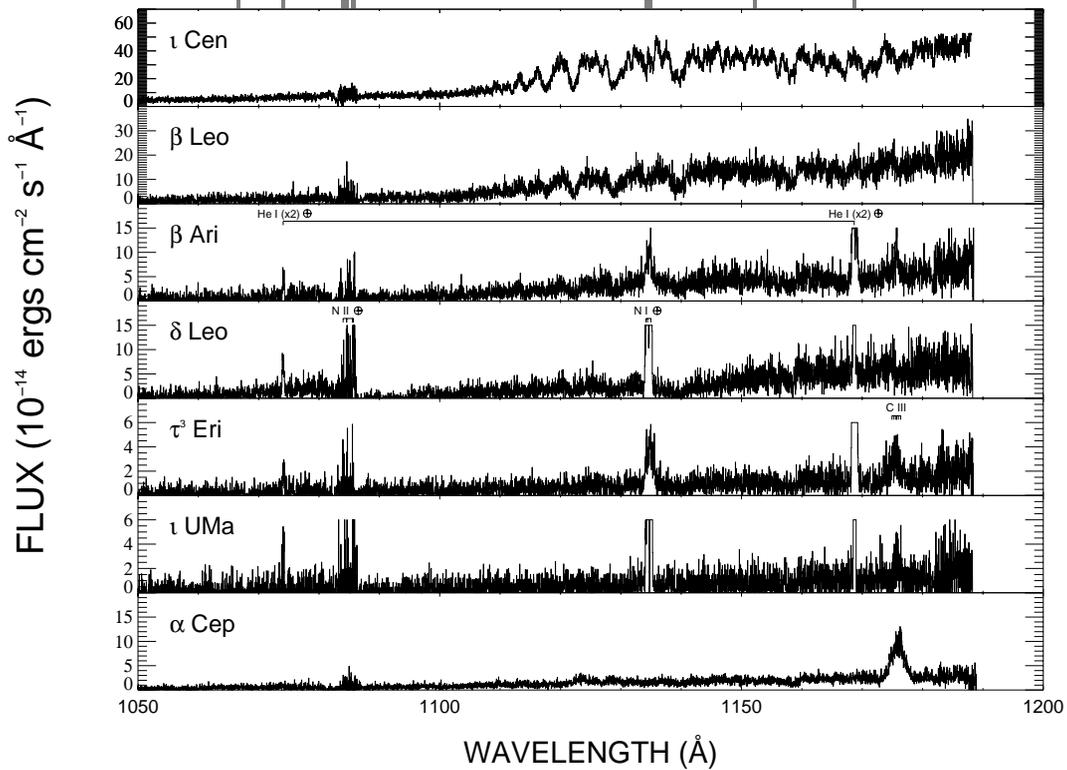[a] Exposure times are averages over individual spectral segments.

Fig. 1a

Fig. 1b

Fig. 1.—*FUSE* spectra of the A star sample, arranged in order of decreasing T_{eff}. (*a*) 905–1050 Å region. (*b*) 1050–1185 Å region. The positions of strong terrestrial airglow lines and of the hydrogen Lyman series are marked in the top panels. The positions of the lines of terrestrial O I are also marked in the middle panel above the spectrum of the chromospherically inactive star δ Leo. The strongest stellar chromospheric lines are identified in the bottom panels. We note that the broad stellar lines are clearly discernible from the much narrower terrestrial lines, e.g., in the wavelength region near the N III lines at 990 Å or at O VI λ1037. The data for α Cep are limited to the nighttime portion of the *FUSE* orbit; the remaining spectra are from the full data sets. Each trace is smoothed to a resolution of 0.05 Å.

TABLE 3
Observed FUV Emission-Line Fluxes

Star	C III 977 Å ($\times 10^{-14}$ ergs cm^{-2} s^{-1})	O VI 1032 Å ($\times 10^{-14}$ ergs cm^{-2} s^{-1})	O VI 1037 Å ($\times 10^{-14}$ ergs cm^{-2} s^{-1})	C III 1175 Å ($\times 10^{-14}$ ergs cm^{-2} s^{-1})
ι Cen	<2.1	<2.1	<3.2	...
β Leo	<1.0	<1.1	<0.5	...
β Ari	5.4 ± 0.7	4.8 ± 0.5	3.3 ± 0.5	5.5 ± 0.8
δ Leo	<1.0	<0.5	<0.2	<2.0
τ^3 Eri.....	5.3 ± 0.9	2.1 ± 0.2	0.9 ± 0.2	3.3 ± 0.5
ι UMa...	8.5 ± 0.9	3.0 ± 0.3	1.5 ± 0.2	1.6 ± 0.3
α Cep	34.0 ± 3.4	10.2 ± 1.0	7.0 ± 1.0	17.9 ± 1.8

Note.—Fluxes at Earth, not corrected for interstellar extinction.

2.3. The HST GHRS Spectra

Emission-line fluxes for two key chromospheric lines outside the *FUSE* spectral range, Si III λ1206 and Lyα λ1215, are available from GHRS spectra of three stars in our *FUSE* sample: τ^3 Eri, ι UMa, and α Cep. Summaries of the observations and results are listed in Table 4. The data were retrieved from the *HST* public archive and calibrated by an "on-the-fly" scheme. Each observation was acquired through the small science aperture ($0\rlap{.}''22 \times 0\rlap{.}''22$, post-COSTAR) and has a resolution of $\lambda/\Delta\lambda \sim 3 \times 10^4$.

Spectra for the three stars are shown in Figure 2, along with a high-quality GHRS spectrum of the A7 dwarf α Aql (Altair), which serves as a comparison. The cores of the broad Lyα features of all four stars are strongly absorbed by interstellar H I; the narrow emission component visible in several of the traces is geocoronal. The observation of ι UMa was centered on the primary star and, in view of the small aperture size, must have excluded the two nearby dM companions. All three stellar components almost certainly were enclosed within the LWRS aperture during our *FUSE* observation of ι UMa. To measure the strength of the Si III feature for this star, as well as for τ^3 Eri, we integrated the net flux over the wavelength interval, 1205–1208 Å. As is evident from Table 4, we obtained only an upper limit for ι UMa. Our result for τ^3 Eri is $\sim$10% lower than the one published earlier from the same spectrum by Simon & Landsman (1997).

2.4. The ROSAT Pointings

X-ray measurements for the stars in our *FUSE* sample, nearly all of them upper limits, are available from the literature (Golub et al. 1983; Schmitt et al. 1985; Simon et al. 1995; Schmitt 1997; Hünsch, Schmitt, & Voges 1998). The provenance of those data is varied, however, reflecting a wide range of detection thresholds. We therefore reexamined material from the *ROSAT* public archive in order to gain a more systematic view of the X-ray properties of the *FUSE* A stars. Table 5 lists the archival data sets that we retrieved using the on-line search engine of the High Energy Astrophysics Science and Archival Research Center (HEASARC) at the NASA Goddard Space Flight Center. Five stars were observed in moderately deep pointings by the Position Sensitive Proportional Counter (PSPC); ι UMa was observed by the High Resolution Imager (HRI); but no X-ray images were found for β Ari.

The event list for each observation was processed using custom software similar to that described by Ayres et al. (1998). Here we took additional steps beyond those required for simple measurements of obvious coronal sources. In particular, we correlated the centroids of all the bright sources in each *ROSAT* field with entries in the *HST* Guide Star Catalog 2.2 in order to rectify small pointing errors (typically $\sim$5″ in size). Applying the pointing offset, we then predicted the location of the *FUSE* A star in the field, taking account of proper motions if necessary. We adopted a 2′ diameter circle to accumulate the source counts, limiting them to the 0.24–2.0 keV energy band, or to establish upper limits based on the average background counts in the vicinity of the target. A description of our background estimation procedure can be found in Ayres et al. (1998). From Monte Carlo simulations, we estimated the 3 σ detection threshold to be $3(1 + N)^{1/2}$, where N is the average number of background counts expected in the source circle.

To convert the measured X-ray count rates or their upper limits to fluxes at Earth, we applied an energy conversion factor (ECF) of 1×10^{-11} ergs cm^{-2} counts^{-1} for the PSPC and 2×10^{-11} ergs cm^{-2} counts^{-1} for the HRI. Those values were estimated using the HEASARC's WebPIMMS flux conversion tool, based on a variety of Raymond-Smith ther-

TABLE 4
HST GHRS Observations

Star Name	*HST* Data Set	UT Date	Exposure Time (ks)	Si III 1206 Å ($\times 10^{-14}$ ergs cm^{-2} s^{-1})	Lyα 1215 Å ($\times 10^{-14}$ ergs cm^{-2} s^{-1})
τ^3 Eri...........	z30c0106t	1996 Feb 10	0.87	8.8 ± 3.5	33.8 ± 5.4
ι UMa	z30c0206t	1996 Feb 19	0.98	<4.9	14.5 ± 4.6
α Cep	z30c0507t	1996 Feb 20	3.26	24.0 ± 1.8	172 ± 4

Note.—Fluxes at Earth, not corrected for interstellar extinction. All exposures are post-COSTAR, in G140M medium-resolution mode, and through the small science aperture.
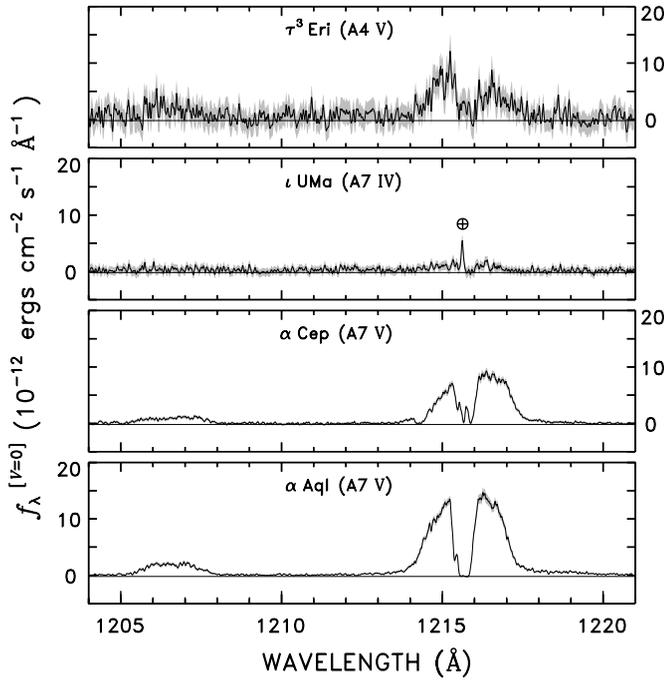
FIG. 2.—Archival GHRS spectra of four A stars in the vicinity of Si III $\lambda 1206$ and Lyα. The individual traces are normalized to $V = 0.0$ for a fair comparison. The shaded areas represent the $\pm 1 \, \sigma$ photometric error bounds. The Altair spectrum is from data set z30c0407t (1996-03-05; 0.76 ks) and is included here for comparison with the three *FUSE* stars in order to demarcate the positions of the Si III and Lyα lines.

mal models. The ECF for the PSPC is relatively insensitive to the source temperature or to abundance depletions for count rates measured within the pulse height channels corresponding closely to our chosen reference energy band of 6–60 Å. The HRI is a different matter because of its lack of any intrinsic energy resolution. It has a low ECF of 0.5×10^{-11} ergs cm^{-2} counts^{-1} for a source temperature of $10^{5.8}$ K, rising to a peak of 2.7×10^{-11} ergs cm^{-2} counts^{-1} at $10^{6.3}$ K and then declining to $\sim 2.1 \times 10^{-11}$ ergs cm^{-2} counts^{-1} at $10^{7.0}$ K. We adopted a representative value of 2×10^{-11} ergs cm^{-2} counts^{-1}, which is appropriate for either a relatively soft, solar-like corona ($T_{\rm cor} \sim 10^{6.2}$ K) or else a relatively hard dMe-like source ($T_{\rm cor} \sim 10^{7.0}$ K).

The X-ray flux or 3 σ upper limit derived for each star is listed in Table 5. With the exception of ι UMa and α Cep, the *FUSE* targets were not detected in the corresponding *ROSAT* fields. ι Cen was undetected in a serendipitous PSPC image at a 3 σ threshold of 0.003 counts s^{-1}. The predicted target position is $17'$ from field center, close to a shadow cast by the inner support ring of the PSPC window. We adopted the nominal upper limit, recognizing that a weak source could be present at a higher intensity but obscured by the low-sensitivity region on the detector.

β Leo technically is a $\gtrsim 2 \, \sigma$ detection at its predicted position in a deep 17 ks PSPC exposure. However, the X-ray field is extremely crowded with sources, increasing the possibility for an accidental detection. Therefore, in place of the measured count rate for this star (0.0007 counts s^{-1}), we adopted the 3 σ threshold of 0.0009 counts s^{-1} as a firm upper limit, pending verification with a higher resolution X-ray pointing.

No pointed observation is available for β Ari, so we estimated an upper limit for that star from its absence in the *ROSAT* Faint Source Catalog[3] (Voges et al. 2000). The typical all-sky survey exposure in the vicinity of β Ari was 0.3 ks (based on cataloged sources within $2°$ of the A star). The average background in the region in the full PSPC energy range (0.1–2.4 keV) is 0.0007 counts s^{-1} arcmin^{-2}. The Faint Source Catalog uses a very conservative $5'$ radius detect circle, which implies a 3 σ detection threshold of 0.04 counts s^{-1}. Converting to our narrower energy range (0.2–2 keV), we estimate the detection threshold to be ~ 0.02 counts s^{-1} for an X-ray source temperature of $10^{6.2}$ K or higher, but less than that if the putative source is softer.

ι UMa was the target of a short 1.8 ks HRI exposure, and a moderately bright source appears near field center. However, the centroid of the source lies $15''$ to the east of the expected position of the primary star, ι UMa A. The displacement is larger than the typical pointing errors we have encountered in HRI images, but unfortunately there are no other bright sources in the field to validate the accuracy of the pointing. Tentatively, we attribute the X-rays to the A star but raise the possibility that the emission may arise

---

[3] See http://www.xray.mpe.mpg.de/rosat/survey/rass-fsc.

TABLE 5
ROSAT OBSERVATIONS

Star Name	*ROSAT* Data Set	UT Date	Exposure Time (ks)	$C_{\rm X}$ (counts ks^{-1})	Flux 6–60 Å ($\times 10^{-14}$ ergs cm^{-2} s^{-1})	Notes
ι Cen	rp600526n00	1993 Jul 11	8.9	<3.3	<3.3	1
β Leo	rp100366n00	1990 Jun 20	17.1	<0.9	<0.9	2
β Ari	...	...	[0.3]	<20	<20	3
δ Leo	rp200213n00	1991 Jun 03	21.5	<1.2	<1.2	
τ^3 Eri...........	rp701503n00	1993 Aug 10	3.4	<3.3	<3.3	
ι UMa	rh200640n00	1991 Nov 05	1.8	47 ± 5	94 ± 10	4
α Cep	rp200211a00	1991 Jul 02	3.7	7.4 ± 1.5	7.4 ± 1.5	
α Cep	rp200211a01	1992 May 17	3.4	9.0 ± 1.7	9.0 ± 1.7	

NOTE.—Count rates for 0.2–2 keV band. Fluxes at Earth, not corrected for interstellar extinction. Upper limits are 3 σ. We adopted an ECF of 1×10^{-11} ergs cm^{-2} counts^{-1} for the PSPC and 2×10^{-11} for the one HRI observation (of ι UMa). The latter is uncertain ($\pm 50\%$), owing to the unknown source temperature. (1) Predicted target position $17'$ from field center, near inner rib of PSPC window. (2) Crowded region. (3) Based on nondetection in All-Sky Survey (Faint Source Catalog). (4) HRI image. Source located $15''$ east of predicted position.

TABLE 6
Normalized Emission Fluxes

Star	T_{eff} (K)	C III 977 Å ($\times 10^{-7}$)	O VI 1032 Å ($\times 10^{-7}$)	O VI 1037 Å ($\times 10^{-7}$)	C III 1175 Å ($\times 10^{-7}$)	Si III 1206 Å ($\times 10^{-7}$)	Lyα 1215 Å ($\times 10^{-7}$)	X Rays 6–60 Å ($\times 10^{-7}$)
ι Cen	8630	<0.10	<0.10	<0.16	...	...	...	<0.16
β Leo	8590	<0.03	<0.03	<0.01	...	...	...	<0.03
β Ari	8400	0.26 ± 0.03	0.23 ± 0.02	0.16 ± 0.02	0.26 ± 0.04	...	...	<1.0
δ Leo	8300	<0.04	<0.02	<0.01	<0.09	...	...	<0.05
τ^3 Eri.....	8210	0.96 ± 0.16	0.38 ± 0.04	0.16 ± 0.04	0.60 ± 0.09	1.6 ± 0.6	6.1 ± 1.0	<0.60
ι UMa ...	8060	0.64 ± 0.07	0.23 ± 0.02	0.11 ± 0.01	0.12 ± 0.02	<0.37	1.1 ± 0.3	7 ± 1
α Cep	7840	1.34 ± 0.13	0.40 ± 0.04	0.28 ± 0.04	0.70 ± 0.07	0.95 ± 0.07	6.8 ± 0.2	0.32 ± 0.08
Sun	5770	1.44	0.73	0.63	0.62	1.12	70	3.7

from a coincidental object, perhaps the pair of dM companions (the BC components). Once again, confirmation from a higher resolution X-ray image is needed.

The deep *ROSAT* measurements of β Leo and δ Leo place the most restrictive limits on coronal X-ray emission among the early A stars in our *FUSE* sample, yielding upper limits on the normalized X-ray flux of $R_{\mathrm{X}} = L_{\mathrm{X}}/L_{\mathrm{bol}} \lesssim 5 \times 10^{-9}$. Here L_{X} is the X-ray luminosity of the star and L_{bol} its bolometric luminosity. The typical X-ray brightness for the Sun and other late-type stars is 2 orders of magnitude larger, $R_{\mathrm{X}}^{\odot} \approx 4 \times 10^{-7}$. Upper limits at much fainter levels are found in late-type stars only among the "noncoronal" red giants, which may represent an evolutionary endpoint in stellar activity (Linsky & Haisch 1979; Ayres, Fleming, & Schmitt 1991). Weak X-ray emission at very faint levels, $R_{\mathrm{X}} = 1-3 \times 10^{-9}$, has been observed for some middle and late B stars (Cassinelli et al. 1994). Cohen, Cassinelli, & MacFarlane (1997) speculate that such cases may represent a transition from shock heating in radiatively driven winds among the O and early B stars to a coronal mechanism at later spectral types. Other late B stars are observed to be much stronger sources, having X-ray luminosities as high as $L_{\mathrm{X}} \approx 10^{31}$ ergs s^{-1} and $R_{\mathrm{X}} \approx 10^{-6}$ (Berghöfer et al. 1997; Huélamo et al. 2000). Several of the X-ray–luminous B stars are known from high-resolution infrared imaging to have close binary companions (Hubrig et al. 2001), which would not have been resolved by *ROSAT* and thus may account for the strong X-ray emission observed.

3. DISCUSSION

We consider first the single stars in the *FUSE* sample, comparing their chromospheric activity levels with those observed for the Sun and other solar-type stars. Table 6 lists the normalized UV line fluxes, i.e., the ratios of the integrated line fluxes to the stellar bolometric luminosities. The equivalent normalized fluxes for the Sun (Ayres 1997) are shown in the last line of the table for comparison. Solar-like values have also been reported by Redfield et al. (2002) for a number of other late-type stars, including, for example, α Cen and α CMi.

The normalized chromospheric line fluxes[4] of the nonbinary A stars are within a factor of 2 of solar values among the reddest stars in our sample, up to a $B-V$ color index of

0.16 and a temperature of $T_{\mathrm{eff}} = 8200$ K (as represented by the star τ^3 Eri). Blueward of that point, among the stars hotter than $T_{\mathrm{eff}} \geq 8300$ K, no chromospheric emission is detected, nor do we find any clear evidence for coronal X-ray emission. The UV detection limits for two of the hotter stars, δ Leo and β Leo, are 30–40 times below solar levels. Thus, within a very narrow temperature range, chromospheric emission drops abruptly from solar brightness levels to more than 1 order of magnitude less. This pronounced change in activity along the main sequence occurs within a temperature range of just ± 50 K, centered on $T_{\mathrm{eff}} \approx 8250$ K. A similar peak and cutoff are present in the acoustic wave fluxes computed for main-sequence stars by Ulmschneider et al. (1999). In that study, and also in work by Gilliland (1986), the predicted wave fluxes rise from low temperatures to a broad maximum near $T_{\mathrm{eff}} = 7750$ K and then decline sharply at higher temperatures, falling by 1 order of magnitude or more at $T_{\mathrm{eff}} = 8300$ K. The sudden downturn in computed wave flux is consistent with stellar structure models. As illustrated by Figure 3 of Christensen-Dalsgaard (2000), at $T_{\mathrm{eff}} = 8300$ K the outer convective regions associated with the ionization of hydrogen and the second ionization of helium are narrow and disjoint (although possibly linked by overshooting; Latour, Toomre, & Zahn 1981), and they transport very little energy compared with radiation. There are, however, a number of limitations to such calculations due to their reliance on mixing-length theory, which provides an incomplete description of convection as compared with hydrodynamical treatments (e.g., Sofia & Chan 1984). For example, in the calculations by Ulmschneider et al., the precise temperature along the main sequence where the acoustic energy curve reaches its peak is subject to considerable uncertainty, as is the magnitude of the predicted wave flux on the high-temperature side of the peak (a point that was acknowledged by those authors). More recent stellar models by Kupka & Montgomery (2002), employing an alternative theory of convection, nonetheless show a similar decline in convective flux, which amounts to 1 order of magnitude or more over the same range in T_{eff} from 7500 to 8500 K. Thus, current theory and our *FUSE* observations appear to be in substantial agreement that along the main sequence there is a rapid decline in chromospheres and convection among the early A stars, which has its onset near $T_{\mathrm{eff}} = 8250$ K.

We turn now to the two binary stars in our sample, β Ari and ι UMa. The former is a spectroscopic binary and was detected at relatively strong UV emission levels by *FUSE*. If the emission originates from the A star primary, the

[4] The identical conclusions apply if the observed emission-line fluxes are stated in terms of fluxes at the stellar surface rather than normalized fluxes.

observed fluxes correspond to approximately one-quarter solar. Our 3 σ upper limit on coronal X rays is roughly 50% solar, but as much as 10 times larger than expected if the X-ray/UV flux ratio of α Cep is used as a guide. Based on the Strömgren photometry, we estimate $T_{\mathrm{eff}} = 8400$ K for the primary, which places the star 150 K above the chromospheric/convective boundary established by the single stars in our *FUSE* sample. We can find no reason to discount the observation of β Ari. We offer four possible explanations to reconcile the apparent contradiction it thus raises.

1. The dividing line for chromospheres and convection is at a higher temperature for binaries than for single stars. Owing to differences in their internal structure, binaries are able to sustain vigorous convection and detectable chromospheres to a higher T_{eff} than single stars.

2. There is no unique location along the main sequence that separates stars having radiative outer envelopes from those having convective ones. For an individual star, the transition between a radiative and a convective envelope is determined by certain structural or physical parameters, whose transformative role has yet to be explicitly identified by observations or theoretical models.

3. Our effective temperature for β Ari is in error. Allende Prieto & Lambert (1999) estimated a lower temperature of 8130 K for β Ari, somewhat cooler than δ Leo and the same as τ^3 Eri. Their estimate would place β Ari below the convective cutoff point near 8200 K and hence eliminate any discrepancy. Sokolov (1995), on the other hand, attributed a lower T_{eff} to β Ari but still ranked it hotter than δ Leo, a star we failed to detect, thereby leaving the two stars out of order on the main sequence in terms of the chromospheric/convection boundary.

4. The primary star is chromospherically inactive, and the UV emission originates entirely from the cooler spectroscopic secondary star. Consequently, the " nondetection " of the A star primary is fully consistent with the trend in the UV emission of the single stars in our sample.

Of the four explanations, the final one appears to us to be the most likely. If we attribute the FUV emission of β Ari entirely to the spectroscopic companion, the normalized chromospheric fluxes would be ~15 times greater than those listed in Table 6 for the primary component. The revised fluxes would then be similar to the values Redfield et al. (2002) obtained for the K0 dwarf ϵ Eri and not unreasonable for an active F, G, or K star. Further suppport for this interpretation comes from the profiles of the FUV emission lines. The widths of C III $\lambda977$ and O VI $\lambda1032$ in the *FUSE* spectrum of β Ari are 10 times smaller than the corresponding widths measured for α Cep and 8–10 times smaller than the widths of Si III $\lambda1206$ in the *HST* spectra of τ^3 Eri, α Cep, and Altair (see Fig. 2). In terms of their FWHM, both lines are less than half as wide as expected from the $\upsilon \sin i$ of the primary, given the factors of 2–3 enhanced broadening that are typically seen in the *FUSE* and *HST* spectra of other A-type stars. Instead, they more closely resemble the much narrower lines of a late-type star, such as α Cen A or B (FWHM ~ 60 km s^{-1}; Wood, Linsky, & Ayres 1997) or Procyon (FWHM ~ 75 km s^{-1}; Wood et al. 1996).

The modest signal-to-noise ratio of our β Ari spectrum stands in the way of a more detailed analysis. At higher signal-to-noise ratio it may be possible to discriminate between an origin at the primary or secondary star if the observed spectral line profile can be decomposed into separate veloc-

ity components. The difference in the orbital velocities of the binary pair at the time of the *FUSE* observation, near an orbital phase of 0.7, is very small (Tomkin & Tran 1987). This is true for most of the orbit because of the high eccentricity. However, when the stars are near periastron, their relative Doppler shift is far larger (~190 km s^{-1}) than the velocity resolution of *FUSE* spectra and the two stars are cleanly separated. For the present, based solely on the line width evidence, we dismiss β Ari as a potential discrepancy with respect to the chromosphere/convection boundary but take note of the fact that the identity of the active star could likely be settled by a single observation with *FUSE* or *HST* if it were timed to coincide with periastron passage.

The second A star binary in our sample, the visual binary ι UMa, has an effective temperature below the chromospheric " cutoff " point. The large aperture of our *FUSE* observation enclosed all three members of the system. Consequently, the extent to which the A star contributed to the observed flux, if at all, cannot be directly determined. Marilli et al. (1997) detected weak Lyα emission in *IUE* spectra of this star, which they attributed to the primary component; however, they used the large aperture ($10'' \times 20''$) of *IUE*, which also must have encircled all three stars. The GHRS observation depicted in Figure 2 was made through the small science aperture and completely isolated the primary star. Compared with α Cep, the Lyα emission in the ι UMa GHRS spectrum is extremely weak (a factor of 6 lower in normalized flux). Moreover, as we saw for β Ari, the emission lines in the *FUSE* spectrum of ι UMa are exceedingly narrow: O VI $\lambda1032$ has an FWHM of only 53 km s^{-1}, which is nearly 5 times smaller than expected for the 140 km s^{-1} rotation velocity of the A star. Nothing can be inferred from the ratios of the FUV line fluxes or their normalized values as to whether the *FUSE* emission originates from the primary star or its late-type companions; the data are compatible with either choice. Assigned to the primary, the observed X-ray flux is a factor of ~70 too high in relation to the *FUSE* line strengths if the ratio of X-ray to FUV brightness follows the trend for other late A and early F stars, including α Cep. Assigned to the dM companions, the X-ray flux is a factor of ~10 too low in comparison with other low-mass stars. Barring significant time variability, the lack of agreement therefore suggests that the X-ray emission and the FUV emission may come from different objects in the field of view.

Again, as with β Ari, we eliminate ι UMa from consideration in defining the chromospheric boundary because most, if not all, of its FUV and/or X-ray emission could plausibly be contributed by its companions. The apparent weakness of its Lyα emission with respect to α Cep and τ^3 Eri must be considered a potential discrepancy, nevertheless. On our stellar temperature scale, or on the scale of Allende Prieto & Lambert (1999), τ^3 Eri is the hottest and most massive A star we have found to exhibit FUV and UV emission: It defines the low-temperature, low-mass *active* side of the chromosphere/convection boundary. C III and O VI emission also is present in the *FUSE* spectrum of β Pic (Deleuil et al. 2001), which has the same T_{eff} as τ^3 Eri (8200 K; Lanz, Heap, & Hubeny 1995), thus reaffirming that main-sequence stars as hot as 8200 K are chromospherically active. The possible inactivity of ι UMa A, at a lower effective temperature, therefore raises the prospect that whether a main-sequence A star is convective or not is a function of a second (thus far hidden) parameter in addition to T_{eff}.

Given the limitations of our small *FUSE* sample, new observations would be needed to test that possibility.

4. CONCLUSIONS

Main-sequence A stars have both a small convective core as well as a thin outer convective zone just below the visible surface. While neither of these two regions is directly observable, convection clearly plays a key role in many aspects of A star behavior. One of the most notable of these is the formation of a high-temperature chromosphere or corona. Using *FUSE*, we have observed the far-UV spectra of a sample of normal A-type stars, which cover a broad range in $T_{\rm eff}$ and color index. Our goal was to use the diagnostic lines of O vi and C iii to determine the locus for the onset of chromospheres, coronae, and convection zones along the main sequence, thereby testing the predictions of stellar structure models and models of chromospheric/coronal heating. Such observations are best made below Lyα, where A star photospheres are much darker than they are at longer wavelengths and therefore less of an obstacle for detecting faint chromospheric emission lines.

Our observations place the boundary line for convection at, or very near, a temperature of 8250 K, with a very steep decline toward hotter temperatures, in general agreement with stellar structure models. Our observational result is subject to uncertainties of ~250 K in the stellar effective temperature scale, based on the scatter found in different standard techniques for estimating $T_{\rm eff}$ (e.g., Castelli et al. 1997; Smalley & Kupka 1997; Allende Prieto & Lambert 1999). It is also affected to an uncertain extent by the rapid rotation of our *FUSE* sample, which may have altered the shapes, photometric colors, and effective temperatures of those stars. According to the models of Collins & Sonneborn (1977), the general consequence of rapid rotation is to shift a star to a lower $T_{\rm eff}$, making it look redder and cooler than a nonrotating star. The changes apparent to an observer are a function of both the rotation speed and the axial inclination of the star. Thus, the colors and $T_{\rm eff}$ of the rapid rotators in our *FUSE* sample may depend on the aspect with which we have viewed them. The resulting effect on each star must then be evaluated on a case-by-case basis, with knowledge of the inclination angle. Unfortunately, the orientations of most stars—including all of the *FUSE* stars—are unknown. The synthetic Strömgren indices for nonrotating and rotating models provided by Collins & Sonneborn (1977) suggest that the differential effects in $T_{\rm eff}$ for our *FUSE* sample could be as large as 500 K; i.e., the true boundary line for the onset of stellar convection may be located higher up the main sequence at ~8800 K rather than at ~8300 K. That estimate follows from applying the same procedure we used to calculate the $T_{\rm eff}$ values in Table 1 (as described in § 2.1). A similar result is obtained from the statistical corrections for rotation derived by Figueras & Blasi (1998), by applying the analytical expressions given in their Table 3 to the individual stars in our *FUSE* sample.[5] Of course, it should be noted that none of the stellar structure models and none of the chromospheric heating predictions cited earlier in this paper for comparison with the *FUSE* observations take account of rotation, their calculations all having been performed for nonrotating stars.

The two potential discrepancies in our identification of the main-sequence chromosphere/convection boundary involve binary stars. A deep spectroscopic observation with *HST* of the Si iii λ1206 and C iii λ1175 lines of ι UMa, plus a modestly deep X-ray image from the *Chandra X-Ray Observatory*, with its superb ~1″ resolution, would give a definitive answer to the question of whether the primary star of ι UMa is active (as we expect from our *FUSE* spectra of single stars) or the FUV emission we have observed should be attributed to the two nearby dM companions (at ~5″ separation). In the second case, the spectroscopic binary β Ari, an observation with either *FUSE* or *HST* at the time of periastron would unambiguously resolve the question of whether the A star primary is active or the emission we have detected with *FUSE* comes from the later-type secondary star.

---

[5] Arranged in the order of decreasing $T_{\rm eff}$ after the correction for rotation, the *FUSE* stars are δ Leo, β Leo, ι Cen, α Cep, β Ari, τ^3 Eri, and ι UMa. At a revised $T_{\rm eff} = 8875$ K, α Cep is the hottest star to show UV emission, while the weakness of Lyα noted earlier for ι UMa remains unexplained.

REFERENCES

Allende Prieto, C., & Lambert, D. L. 1999, A&A, 352, 555
Ayres, T. R. 1997, J. Geophys. Res. Planets, 102, 1641
Ayres, T. R., Fleming, T. A., & Schmitt, J. H. M. M. 1991, ApJ, 376, L45
Ayres, T. R., Simon, T., Stern, R. A., Drake, S. A., Wood, B. E., & Brown, A. 1998, ApJ, 496, 428
Berghöfer, T. W., Schmitt, J. H. M. M., Danner, R., & Cassinelli, J. P. 1997, A&A, 322, 167
Cassinelli, J. P., Cohen, D. H., MacFarlane, J. J., Sanders, W. T., & Welsh, B. Y. 1994, ApJ, 421, 705
Castelli, F., Gratton, R. G., & Kurucz, R. L. 1997, A&A, 318, 841
Christensen-Dalsgaard, J. 2000, in ASP Conf. Ser. 210, Delta Scuti and Related Stars, ed. M. Breger & M. H. Montgomery (San Francisco: ASP), 187
Cohen, D. H., Cassinelli, J. P., & MacFarlane, J. J. 1997, ApJ, 487, 867
Collins, G. W., II, & Sonneborn, G. H. 1977, ApJS, 34, 41
Cuntz, M., Rammacher, W., & Ulmschneider, P. 1994, ApJ, 432, 690
Deleuil, M., et al. 2001, ApJ, 557, L67
Drake, S. A., Linsky, J. L., Schmitt, J. H. M. M., & Rosso, C. 1994, ApJ, 420, 387
Eggen, O. J. 1956, AJ, 61, 405
Feldman, P. D., Sahnow, D. J., Kruk, J. W., Murphy, E. M., & Moos, H. W. 2001, J. Geophys. Res. A, 106, 8119
Figueras, F., & Blasi, F. 1998, A&A, 329, 957
Gilliland, R. L. 1986, ApJ, 300, 339
Golub, L., Harnden, F. R., Jr., Maxson, C. W., Rosner, R., Vaiana, G. S., Cash, W., Jr., & Snow, T. P., Jr. 1983, ApJ, 271, 264

Gray, R. O., & Garrison, R. F. 1987, ApJS, 65, 581
———. 1989, ApJS, 70, 623
Grillo, F., Sciortino, S., Micela, G., Vaiana, G. S., & Harnden, F. R., Jr. 1992, ApJS, 81, 795
Hubrig, S., Le Mignant, D., North, P., & Krautter, J. 2001, A&A, 372, 152
Huélamo, N., Neuhäuser, R., Stelzer, B., Supper, R., & Zinnecker, H. 2000, A&A, 359, 227
Hünsch, M., Schmitt, J. H. M. M., & Voges, W. 1998, A&AS, 132, 155
Kupka, F., & Montgomery, M. H. 2002, MNRAS, 330, L6
Landsman, W. B. 1993, in ASP Conf. Ser. 52, Astronomical Data Analysis Software and Systems II, ed. R. J. Hanisch, R. J. V. Brissenden, & J. Barnes (San Francisco: ASP), 246
Lanz, T., Heap, S. R., & Hubeny, I. 1995, ApJ, 447, L41
Latour, J. 1970, A&A, 9, 277
Latour, J., Toomre, J., & Zahn, J.-P. 1981, ApJ, 248, 1081
Linsky, J. L., & Haisch, B. M. 1979, ApJ, 229, L27
Marilli, E., Catalano, S., Freire Ferrero, R., Gouttebroze, P., Bruhweiler, F., & Talavera, A. 1997, A&A, 317, 521
Moon, T. T., & Dworetsky, M. M. 1985, MNRAS, 217, 305
Moos, H. W., et al. 2000, ApJ, 538, L1
Pan, X. P., Shao, M., Colavita, M. M., Mozurkewich, D., Simon, R. S., & Johnston, K. J. 1990, ApJ, 356, 641
Parker, E. N. 1970, ARA&A, 8, 1
Peterson, R. C., & Schrijver, C. J. 1997, ApJ, 480, L47
Redfield, S., Linsky, J. L., Ake, T. B., Dupree, A. K., & Young, P. R. 2002, ApJ, in press

Richer, J., Michaud, G., & Proffitt, C. 1992, ApJS, 82, 329
Sahnow, D. J., et al. 2000, ApJ, 538, L7
Schmitt, J. H. M. M. 1997, A&A, 318, 215
Schmitt, J. H. M. M., Golub, L., Harnden, F. R., Jr., Maxson, C. W., Rosner, R., & Vaiana, G. 1985, ApJ, 290, 307
Schmitt, J. H. M. M., Zinnecker, H., Cruddace, R., & Harnden, F. R., Jr. 1993, ApJ, 402, L13
Simon, T., & Ayres, T. R. 1998, ApJ, 500, L37
Simon, T., Drake, S. A., & Kim, P. D. 1995, PASP, 107, 1034
Simon, T., & Landsman, W. B. 1991, ApJ, 380, 200
———. 1997, ApJ, 483, 435
Smalley, B., & Kupka, F. 1997, A&A, 328, 349
Sofia, S., & Chan, K. L. 1984, ApJ, 282, 550
Sokolov, N. A. 1995, A&AS, 110, 553
Tomkin, J., & Tran, H. 1987, AJ, 94, 1664
Ulmschneider, P., Theurer, J., Musielak, Z. E., & Kurucz, R. 1999, A&A, 347, 243
Van Biesbroeck, G. 1974, ApJS, 28, 413
Voges, W., et al. 2000, ROSAT All-Sky Survey Faint Source Catalog (Garching: MPI)
Wood, B. E., Harper, G. M., Linsky, J. L., & Dempsey, R. C. 1996, ApJ, 458, 761
Wood, B. E., Linsky, J. L., & Ayres, T. R. 1997, ApJ, 478, 745
Worley, C. E. 1962, AJ, 67, 403
Young, P. R., Dupree, A. K., Wood, B. E., Redfield, S., Linsky, J. L., Ake, T. B., & Moos, H. W. 2001, ApJ, 555, L121